Solvation shell dynamics of supercritical water–cyclohexane mixtures in relation to the translational and rotational dynamics as studied by molecular dynamics simulation

Cite as: AIP Advances 11, 075219 (2021); doi: 10.1063/5.0057093
Submitted: 17 May 2021 • Accepted: 1 July 2021 •
Published Online: 16 July 2021

Ken Yoshida[a] and Haruka Yoshioka

AFFILIATIONS

Department of Applied Chemistry, Graduate School of Technology, Industrial and Social Sciences, Tokushima University, 2-1 Minamijyousanjima-cho, Tokushima 770-8506, Japan

[a]Author to whom correspondence should be addressed: yoshida.ken@tokushima-u.ac.jp

ABSTRACT

The translational dynamics of water and cyclohexane in supercritical binary mixtures were investigated using molecular dynamics simulations. The effects of the local composition were examined through a decomposition scheme of the conditional time-correlation functions based on the solvation numbers for water and cyclohexane. The self-diffusion of water was found to be largely controlled by the continuous and collective attractive interactions with surrounding water molecules, while interactions with cyclohexane have minimal impact on water diffusion. On the other hand, the self-diffusion of cyclohexane is dominantly determined by uncorrelated collisional interactions with neighboring cyclohexane molecules. The results demonstrate the dynamic aspect of microscopic inhomogeneity and highlight the significance of interactions between molecules of the same species. An examination of the dependence of self-diffusion on the lifetime of the solvation shell indicated that the self-diffusion of water is confined within the solvation shell. This is attributed to the hydrogen bond interactions with neighboring water molecules, which create an energy barrier to the water molecules diffusing out of the hydration cage. In contrast, diffusing cyclohexane molecules migrate beyond the solvation shell, particularly at large water contents.

I. INTRODUCTION

Supercritical water is a green alternative to conventional organic solvents for chemical reactions.[1–3] One of the key properties of supercritical water is its high dissolving power for nonpolar organic species, which cannot be achieved by water under ambient conditions. When a hydrophobic species is dissolved in water and is in contact with water molecules, the partial charges of the solvent water molecules, which would otherwise be shielded at room temperature and pressure, are exposed to the solute. This often induces novel reactions that cannot be realized under ambient conditions.[4–8] To better understand the mechanisms of these reactions, it is important to scrutinize the dynamic interactions between water and nonpolar species. These interactions can be considered as encounters between reactants where the reactive atomic sites make contact for a finite time, which is a prerequisite for chemical reactions to occur. At supercritical temperatures of practical interest of around 400 °C, the attraction between a pair of water molecules persists in pure water, even though the hydrogen bonding (H-bonding) is no longer strong enough to maintain the three-dimensional network structure; this allows water to accommodate hydrophobic solutes.[9–13] In water–hydrophobe mixtures at high temperatures, the association between water molecules should compete with thermally enhanced random diffusion, which acts to keep unlike components intermixed. To characterize this unique aspect of water and hydrophobe molecules under miscible conditions, it is essential to elucidate how the dynamics of the solute are controlled by the structure of the surrounding solute and solvent molecules and its fluctuations over time.

Experimental examinations of mixed water/hydrophobe systems are scarce, although a few have been conducted over a wide range of compositions. In a recent study, we used a

high-temperature nuclear magnetic resonance (NMR) method to investigate the self-diffusion of water and cyclohexane in their binary mixture under supercritical conditions as a function of temperature T, total density ρ, and the mole fraction of water x_w.[13] Cyclohexane was employed as a representative nonpolar organic solvent. The activation energies E_a and activation volumes $\Delta V^{\ddagger}$ for the self-diffusion coefficients of water and cyclohexane were determined over a wide range of x_w, and the effects of H-bonds were highlighted based on the dependency of E_a and $\Delta V^{\ddagger}$ on x_w. Examining the dynamics as a function of x_w and ρ can provide insight into the effects of hydration because variations in the number density of water molecules in the system resulting from variations in x_w or ρ are correlated with the average hydration number around a water molecule. One of the most characteristic features in terms of the peculiarities of water diffusion revealed in the previous study was the remarkably large E_a for water diffusion at large x_w, which implies that neighboring water molecules create a barrier to water diffusion.[13] Deeper insights are still needed to determine the effects of fluctuations in the local composition and density around the diffusing solute molecule as well as their retention and transition over time. These microscopic properties are typically averaged as a function of only macroscopic variables. Thus, it is of particular interest to elucidate the distribution of microscopic variables over a wide range of local structural and dynamic variables because phenomena with low probabilities of occurrence, particularly those controlled by rare events such as chemical reactions, could have important effects. A previous analysis of radial distribution functions illustrated that the preferential association between molecules of the same species is maintained at microscopic length scales for intermolecular distances, even under macroscopically fully miscible conditions at supercritical temperatures above 400 °C.[13] The current study provides insights into such microscopic inhomogeneities related to the structure and lifetime of the solvation shell in supercritical mixtures based on molecular dynamics (MD) simulations. Once the accuracy of the MD interaction potentials is verified by agreement between simulation and experiment, the analysis of MD trajectories becomes a powerful method to reveal phenomena that are averaged in experimental observations. In a previous study, we demonstrated that classical MD simulations can reproduce NMR-determined self-diffusion coefficients to within a few percent.[13]

The analysis in this study is based on a scheme to decompose the time-correlation function of interest into components of the solvation structure and relate it to the lifetime of the solvation shell. This scheme was introduced in a previous study for one-component supercritical fluids[14] and is generalized here for multicomponent systems. The advantage of this scheme is its applicability to supercritical states with a wide range of densities from gas-like low-density states to liquid-like high-density states. This is in distinct contrast to the Brownian model for liquids and the binary collision model for dilute gases. In our scheme, a dynamic feature of interest is characterized based on its relationship with the lifetime of the solvation shell. When the time scale of the dynamic feature of interest is shorter than the lifetime of the solvation shell, the dynamic feature is considered as confined within the shell. Conversely, when the time scale of the dynamic feature of interest is greater than the lifetime of the solvation shell, the solvation shell is considered to be more mobile than the dynamic feature of interest. We denote the former and latter dynamics as "in-shell" and "mobile-shell" types, respectively. Importantly, the two extrema of the in-shell and mobile-shell types correspond to the Brownian model for liquids and the binary collision model for dilute gases, respectively. Our analysis scheme can continuously evaluate the scenarios that lie between these extrema, which typically occur in the medium-density region for supercritical fluids. The scheme was first applied to the translational and rotational dynamics of water and organic solvents[14] and successfully provided a molecular interpretation for the experimental results obtained by high-temperature/high-pressure NMR spectroscopy.[10–12,15,16] The results highlighted the persistence of H-bonds in water in supercritical states.[9,17] The scheme was subsequently applied to analyze the line shapes of vibrational spectra for supercritical water. The number of H-bonds controlled the O–H vibrations of water in supercritical states, which are of the in-shell type, and was a determining factor in the frequency and shape of the broad rotational sideband in the vibrational spectrum.[18,19]

The effects of the persisting H-bonds in supercritical states have attracted significant attention in recent years from both static and dynamic perspectives, and both experimental and computational approaches have been applied to study these effects.[20–30] A recent neutron-scattering study revealed signs of the presence of H-bonding at high temperatures up to 823 K.[31] Here, we reveal the effects of H-bonding in the presence of hydrophobic cyclohexane by analyzing the dynamic solvation shell. Our scheme is particularly powerful for water–cyclohexane mixtures as it can unambiguously identify and categorize solvation shells comprising highly contrasting combinations of species from both structural and dynamic perspectives. Our scheme is free from assumptions about time scale separation and thus allows the continuous exploration of both density and local composition.

Section II describes the procedures used for the MD simulations and summarizes the analysis scheme for the time-correlation functions and relaxation times. Section III analyzes and discusses the solvation shell relaxation, self-diffusion, and rotation of water and cyclohexane in their binary mixtures in supercritical states. Section IV presents the conclusions drawn from the results.

II. PROCEDURES

A. MD simulations

Classical MD simulations were performed for various water–cyclohexane mixtures as described elsewhere[13] with minor modifications. The total number of water and cyclohexane molecules was set to 2000 in all simulations. The total number density, ρ, which is the sum of the molarity of water, ρ_w, and that of cyclohexane, ρ_{ch}, was set to 1.0 or 4.0 M (M = mol dm^{-3}). The mole fraction of water, x_w, was varied from 0.1 to 0.9 in increments of 0.2 at 1.0 M and increments of 0.4 at 4.0 M. The temperature θ was set to 400, 600, and 800 °C. The extended simple point charge (SPC/E)[32] and the optimized potential for liquid simulations-all atom (OPLS-AA)[33] models were used as the pair potential functions for water and cyclohexane, respectively. The SPC/E model is one of the most frequently employed models to simulate water in sub- and super-critical states[22,34–39] because its critical constants (T_c = 651.7 K, ρ_c = 0.326 g cm^{-3}, and p_c = 22.055 MPa)[40] are close to the experimental values (T_c = 647.096 K, ρ_c = 0.322 g cm^{-3}, and p_c = 22.064 MPa).[41,42] The OPLS-AA model has successfully

reproduced the self-diffusion coefficient for cyclohexane in binary mixtures with water in supercritical states[13] and for benzene in sub- and super-critical conditions.[12,16] For each condition, we performed a 30-ns MD simulation using the GROMACS 2019.6 simulation software package[43] with a time step of 1.0 fs following an equilibration run of 1.0 ns.

B. Solvation shell decomposition and lifetime

The analysis scheme is an extension of the dynamic solvation shell analysis for one-component systems[14] to the binary system examined in this study. The solvation number n is employed to specify the state of the solvation shell. The solvation number, which is defined based on the distances between the centers of mass for a pair of molecules, is a universal and versatile criterion for characterizing and comparing the solvation shells of unlike species (e.g., water and cyclohexane) that differ significantly in their structure, size, and interactions. The solvation number n for a given molecule is equal to the number of molecules whose distances are less than the cutoff distance r_c. The cutoff distance r_c was taken to be 4.5, 8.5, and 6.5 Å for water–water, cyclohexane–cyclohexane, and water–cyclohexane pairs, respectively. These values are set so that the first peak of the corresponding radial distribution function is included in the solvation shell. Such radial distribution functions were examined in a previous paper.[13] Investigations of the number of H-bonds determined from the O–H site–site radial distribution functions in a water–cyclohexane mixture[13] and in pure water[14] have shown that the center-of-mass radial distribution function for water pairs reflects the attractive interactions between water molecules due to H-bonds.

For the solvation number of a solute in a binary mixture, the solvation shell is characterized by a combination of the number of molecules of the same and different species of the solute molecule. For a mixture of components A and B, the state of the solvation shell around molecule A is specified by the combination of the number of solvent A molecules $n_{A(A)}$ and the number of solvent B molecules $n_{B(A)}$ around a molecule of solute A. The labels of the species in and before the parentheses in the subscript of n indicate the solute and the solvent, respectively. Hereafter, we refer to $n_{A(A)}$ and $n_{B(A)}$ as the self- and cross-solvation numbers of A, respectively. Water and cyclohexane are indicated by the labels "w" and "ch," respectively.

The dynamics of the solvation shell structure are investigated through a characteristic function, $\Theta_{m,n}(t)$, of self- and cross-solvation numbers; here, the subscripts m and n indicate self- and cross-solvation numbers, respectively. At time t, $\Theta_{m,n}(t)$ is unity when the self-solvation number is equal to m and the cross-solvation number is equal to n, and $\Theta_{m,n}(t)$ is zero otherwise. The characteristic function of a solvation shell in a binary mixture is expressed as

$$\begin{aligned}\Theta_{m,n}(t)\Theta_{j,k}(t) &= \Theta_{m,n}(t) \quad (m = j \text{ and } n = k)\\ &= 0 \quad (m \neq j \text{ or } n \neq k),\end{aligned} \tag{1}$$

$$\sum_m \sum_n \Theta_{m,n}(t) = 1, \tag{2}$$

where the subscripts (m, n) and (j, k) represent the set of self- and cross-solvation numbers, respectively. The dynamic aspect of the solvating molecules is examined in terms of the autocorrelation function for $\Theta_{m,n}(t)$, whose normalized form $C_{m,n}(t)$ is expressed as

$$C_{m,n}(t) = \frac{\langle \Theta_{m,n}(t)\Theta_{m,n}(0)\rangle}{\langle \Theta_{m,n}^2\rangle} = \frac{\langle \Theta_{m,n}(t)\Theta_{m,n}(0)\rangle}{\langle \Theta_{m,n}\rangle}. \tag{3}$$

The second equality in Eq. (3) comes from the definition of $\Theta_{m,n}$ as either zero or unity. The function $C_{m,n}(t)$ is unity at time 0 and decays to the ensemble average $\langle \Theta_{m,n}\rangle \equiv \langle \Theta_{m,n}(0)\rangle$. The average $\langle \Theta_{m,n}\rangle$ is the probability $P_{m,n}$ of finding a molecule with self- and cross-solvation numbers equal to m and n, respectively. The relaxation time $\tau_S(m,n)$ for the solvation shell is obtained by the exponential fit of the initial decay of $C_{m,n}(t)$. The range of $C_{m,n}(t)$ used for the fitting was set to be 0.3 at most and to be larger than half of the difference of the long-time limit, i.e., $\langle \Theta_{m,n}\rangle = P_{m,n}$, from unity. For this purpose, for $\langle \Theta_{m,n}\rangle \leq 0.4$, the region where $C_{m,n}(t) \geq 0.7$ is used for the fitting, and for $\langle \Theta_{m,n}\rangle > 0.4$, $C_{m,n}(t)$ is fit until $C_{m,n}(t)$ reaches $1/2(C_{m,n}(0) + C_{m,n}(\infty)) = 1/2(1 + \langle \Theta_{m,n}\rangle)$.

The translational and rotational dynamics are investigated based on the relaxation time of the translational diffusion (τ_D) and the second-order reorientational correlation time (τ_{2R}), respectively. The τ_D and τ_{2R} values are calculated by integrating the associated autocorrelation functions as follows, respectively:

$$\tau_D = \int_0^\infty \mathrm{d}t \frac{\langle \mathbf{v}(0)\cdot\mathbf{v}(t)\rangle}{\langle \mathbf{v}(0)^2\rangle}, \tag{4}$$

$$\tau_{2R} = \int_0^\infty \mathrm{d}t \left\langle \frac{3}{2}\cos^2\theta(t) - \frac{1}{2}\right\rangle, \tag{5}$$

where $\mathbf{v}(t)$ is the velocity of the center of mass of a molecule at time t and $\theta(t)$ is the angle between the O–H and equatorial C–H bond vectors for water and cyclohexane, respectively. The differences between the τ_{2R} values for the axial and equatorial C–H bonds are within 1% due to the negligibly small effect of anisotropy for nonpolar cyclohexane at the high temperatures studied here and thus do not affect the present discussions. The dependence of τ_D and τ_{2R} on the self- and cross-solvation numbers is examined through the corresponding correlation functions conditioned by m and n at time 0. The τ_D and τ_{2R} values conditioned by $\Theta_{m,n}$ are expressed as

$$\tau_D(m,n) = \int_0^\infty \mathrm{d}t \frac{\langle \mathbf{v}(0)\mathbf{v}(t)\Theta_{m,n}(0)\rangle}{\langle \mathbf{v}(0)^2\Theta_{m,n}(0)\rangle}, \tag{6}$$

$$\tau_{2R}(m,n) = \int_0^\infty \mathrm{d}t \frac{\left\langle \left(\frac{3}{2}\cos^2\theta(t) - \frac{1}{2}\right)\Theta_{m,n}(0)\right\rangle}{\langle \Theta_{m,n}(0)\rangle}. \tag{7}$$

The average of the components for a conditioned relaxation time $\tau_X(m,n)$ ($X = S, D, 2R$) over m and n is the relaxation time at a specific thermodynamic state, which is expressed as

$$\tau_X = \sum_m \sum_n \langle \Theta_{m,n}\rangle \tau_X(m,n) = \sum_m \sum_n P_{m,n}\tau_X(m,n). \tag{8}$$

Equation (8) is the "sum rule" in the description of the decomposition based on the solvation numbers. We also refer to the averaged correlation time τ_X as the bulk material and the solvation-number-conditioned time $\tau_X(m,n)$ as the conditioned material.

To evaluate the uncertainty of the correlation times, the 30-ns MD trajectory at each thermodynamic state is divided into

30 trajectories, and the correlation time conditioned using the solvation numbers is calculated for every 1-ns trajectory. The uncertainty for each correlation time is evaluated based on the standard deviation of the mean for the correlation times of the 30 divisions with a 95% confidence limit. The uncertainty of the solvation-number-conditioned activation energy E_a is evaluated based on the standard deviation of the slope from the Arrhenius plot with a 95% confidence limit.

III. RESULTS AND DISCUSSION

A. Solvation shell structure and dynamics

We first examine the structure and dynamics of the solvation shell in a binary mixture of water and cyclohexane in supercritical states. Figure 1 shows a typical distribution of the probability $P_{m,n}$ in an equimolar mixture ($x_w = 0.5$) of water and cyclohexane at 400 °C and 1.0 M. The probabilities for the solvation shell around water (w) and cyclohexane (ch) are plotted in panels (a) and (b), respectively. We examine the extent to which the states of the solvation shells are gas-like at such low densities and the extent to which the solute is subject to collective and continuous interactions with neighboring molecules. In the present framework based on the solvation numbers, the gas-like state of a system is characterized as the dominant number of molecules in an isolated state where both the self- and cross-solvation numbers are zero or in the middle of a binary interaction where either of the self- or cross-solvation number is one and the other is zero. In terms of probability, this situation corresponds to a case where the sum of $P_{0,0}$, $P_{1,0}$, and $P_{0,1}$ is close to unity and the probability of the other combinations of solvation numbers occurring is negligible. For water, the values of $P_{0,0}$, $P_{1,0}$, and $P_{0,1}$ are 0.59, 0.18, and 0.13, respectively, which means that 90% of water molecules are in a gas-like state; the probabilities in the linear scale are shown in Fig. S1 in the supplementary material. The remaining 10% are surrounded by multiple molecules, and this portion is not small enough to be considered negligible. Compared to water, there is a greater probability of finding a molecule with multiple

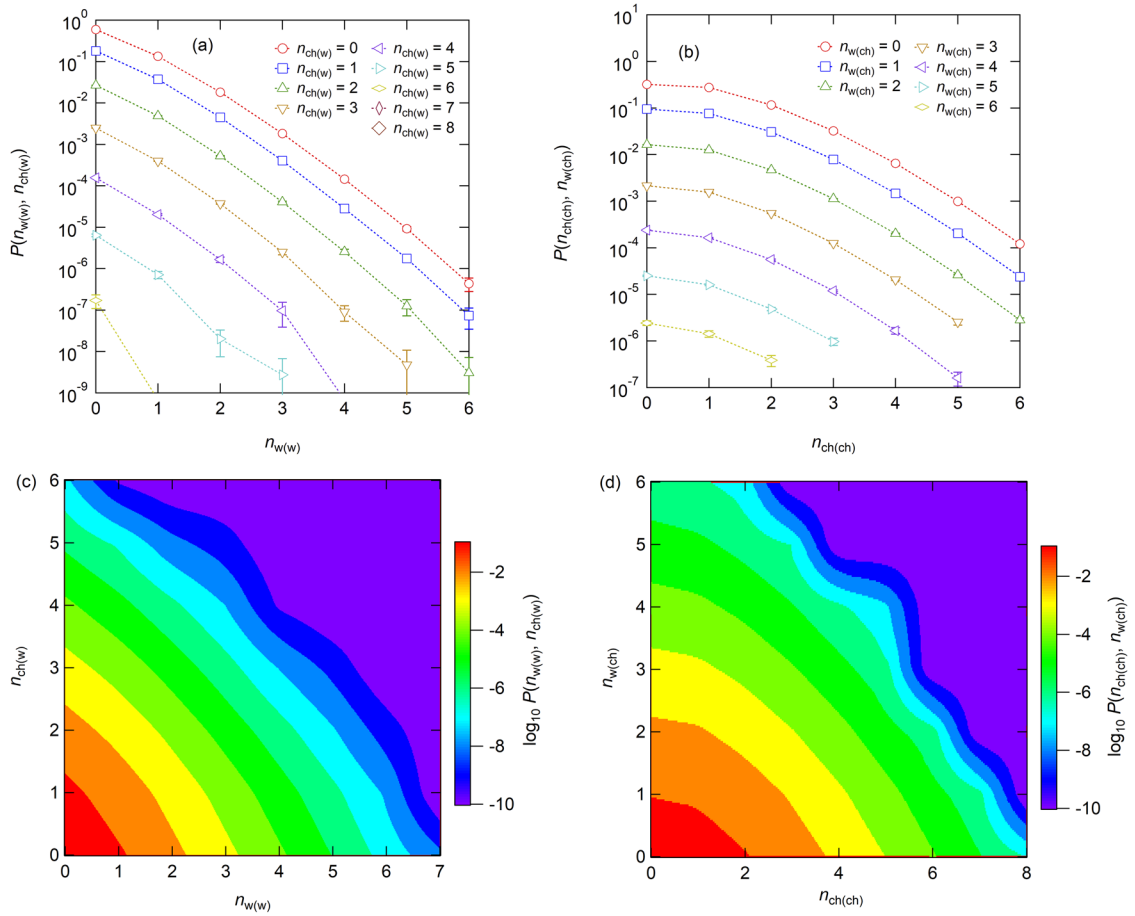

FIG. 1. (a) Probability $P(n_{w(w)}, n_{ch(w)})$ of finding a water molecule with $n_{w(w)}$ surrounding water molecules and $n_{ch(w)}$ surrounding cyclohexane molecules within the solvation shell. (b) The probability $P(n_{ch(ch)}, n_{w(ch)})$ of finding a cyclohexane molecule with $n_{ch(ch)}$ surrounding cyclohexane molecules and $n_{w(ch)}$ surrounding water molecules within the solvation shell. The thermodynamic state is at 1.0 M, 400 °C, and $x_w = 0.5$. (c) Same as (a) but illustrated as a contour plot. (d) Same as (b) but illustrated as a contour plot.

molecule types in its solvation shell for cyclohexane; the fraction of cyclohexane molecules with multiple solvent molecules is 31%. In this respect, the molecules are subject to significant continuous and collective interactions with surrounding molecules, even though many are in the gas-like isolated or binary-interacting states.

The uncertainties of the correlation times conditioned by the solvation number indicate that those with probabilities larger than 10^{-4} can be determined with uncertainties smaller than 10%. This is a rough threshold to indicate whether a quantitative discussion is meaningful based on the statistics of the trajectory sampling for the present MD simulations. A typical example of the relationship between the uncertainty and probability is shown in Fig. S2. There are several solvation states with multiple solvents whose probabilities of occurrence exceed 10^{-4}, as seen from the probabilities in Fig. 1. Therefore, this thermodynamic state is a condition in which the gas-like and liquid-like solvated states coexist. The dynamics of these solvation states can be compared and discussed as described below. The summation of $\tau_D\left(n_{w(w)}, n_{ch(w)}\right)$ weighted by $P(n_{w(w)}, n_{ch(w)})$ over the range of solvation numbers with $P(n_{w(w)}, n_{ch(w)})$ larger than 10^{-4} accounts for 99.99% of the unconditioned bulk τ_D. This means that in the physical discussions below, we can safely neglect the decomposed components with $P(n_{w(w)}, n_{ch(w)})$ less than 10^{-4} or correlation times with uncertainties exceeding 10%. At a higher density of 4.0 M, the probability of finding a molecule surrounded by multiple solvent molecules is 64% and 94% for water and cyclohexane, respectively. The probabilities of the solvation states are shown in Fig. S3. The molecules are accordingly subject to more collective and continuous interactions at higher densities. The average values of the solvation number obtained using these probability distributions are shown in Table SI.

The relaxation times τ_S of the solvation shell for water and cyclohexane are shown in Figs. 2(a) and 2(b), respectively, at θ = 400 °C, ρ = 1.0 M, and x_w = 0.5. In the regions with smaller solvation numbers (less than or equal to 2), the conditioned relaxation time $\tau_S(m,n)$ decreases as the self- and cross-solvation numbers increase. Such a decrease in τ_S with increasing n is common for pure solvents of water and benzene, as studied previously.[14] This decrease occurs because there are more chances for the solvation shell with a larger number of molecules to be involved since the changes in the states of the solvation shell are caused by a solvent molecule leaving the solvation shell or the coming in of an additional molecule. For exiting molecules, the number of candidates that leave increases when more solvating molecules are present in the shell, and the effect of molecules entering into the solvation shell decreases when there are already a larger number of molecules present.

These trends are common in water-rich (x_w = 0.9) and water-poor (x_w = 0.1) conditions (Fig. S4). It is noted that the rate of decrease in τ_S with increasing n becomes smaller at large n. At a higher density of 4.0 M, where the occurrence of larger n is more probable, τ_S increases with increasing n, as observed in Fig. S5. Such an increase in τ_S with n at large n has not been observed in one-component systems.[14] The solvation states where such increments in τ_S are observed are in a condition where solvent molecules are highly clustering around a solute molecule for the thermodynamic state. Although the occurrence of such solvation states is rare, a long lifetime indicates that once a cluster is created, it tends to be stable and resistant to disintegration into isolated monomers. The presence of microscopic inhomogeneity due to molecular-level affinity between the same species has been described by inspecting the static radial distribution function.[13] These findings demonstrate the origin of microscopic inhomogeneity from a dynamics perspective by showing that the microscopic inhomogeneity can be attributed to the clustering of water molecules driven by H-bonding. The non-conditioned, average values of τ_S are listed in Table SII, along with those of τ_D and τ_{2R}.

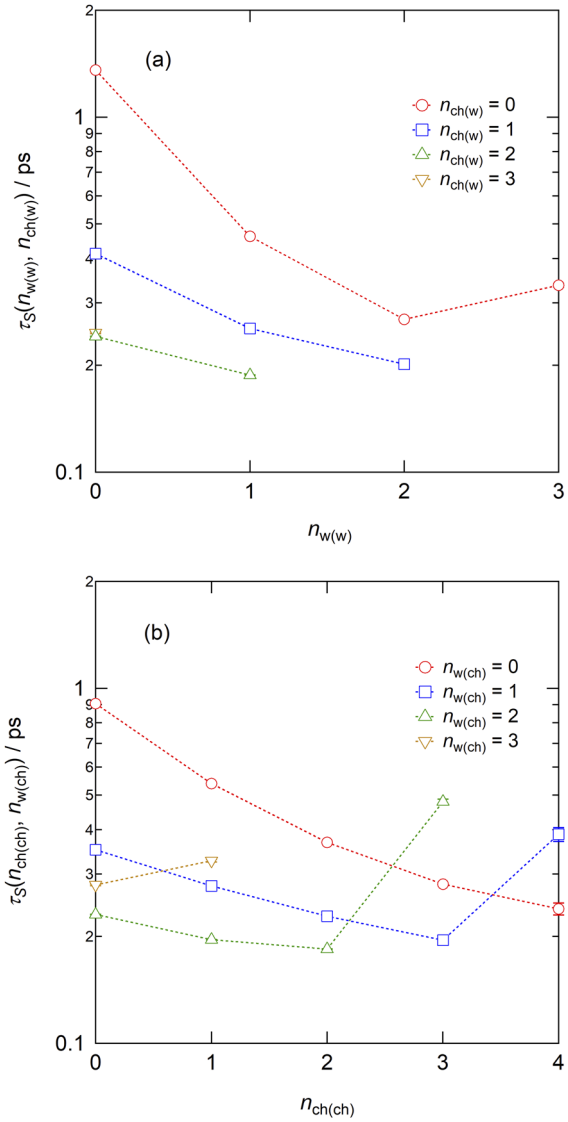

FIG. 2. (a) Relaxation time $\tau_S\left(n_{w(w)}, n_{ch(w)}\right)$ for the solvation shell of water as a function of the number $n_{w(w)}$ of solvating water molecules. (b) The relaxation time $\tau_S\left(n_{ch(ch)}, n_{w(ch)}\right)$ for the solvation shell of cyclohexane as a function of the number $n_{ch(ch)}$ of solvating cyclohexane molecules. The thermodynamic state is at 1.0 M, 400 °C, and x_w = 0.5.

B. Translational dynamics

Here, we consider how the translational dynamics of water and cyclohexane are controlled by the solvation shell structure. We examine how the velocity relaxation time τ_D depends on the solvation numbers of water and cyclohexane and how they are related to the relaxation time of the solvation shell. Figure 3 shows the solvation-number-conditioned velocity relaxation times for water $[\tau_D(n_{w(w)}, n_{ch(w)})]$ and cyclohexane $[\tau_D(n_{ch(ch)}, n_{w(ch)})]$ at 400 °C, 1.0 M, and x_w = 0.5. We first examine the results for water in Fig. 3(a), which shows that τ_D decreases with either $n_{w(w)}$ or $n_{ch(w)}$. As the density is low in this condition, the effect of the solvating water is attributed to the attractive interactions rather than the repulsive interactions that operate in dense fluids. When the number of neighboring H-bonding partners is larger, the randomization of the velocity correlation is accelerated for the diffusing solute water molecules by H-bonding interactions. The influence of solvating cyclohexane molecules on the diffusion of water is also noticeable in Fig. 3(a). From a static perspective of the solvation structure, we showed previously that water and cyclohexane avoid each other in high-temperature mixtures, as seen in the lower height of the first peak of the water–cyclohexane radial distribution function compared to those for the same species.[13] This indicates that water molecules prefer avoiding direct contact with cyclohexane molecules on average; however, once water encounters cyclohexane, the diffusion of water is slowed by the attractive van der Waals interactions and the repulsive forces from cyclohexane molecules. The translational path of water diffusion in the direction straight ahead is obstructed by the heavier and bulkier cyclohexane molecules, and the attraction between water and cyclohexane should have additional effects. Comparing the effects of the solvating water and cyclohexane molecules indicates that the effect of water molecules is more significant than that of cyclohexane. The ratio at which τ_D for water is reduced per one increment of $n_{w(w)}$ is 20%–30%, which is larger than the 10%–20% reduction in τ_D for each increment of $n_{ch(w)}$. The effects of water–water attractive interactions revealed here are remarkable and more than offset by the fact that water is a much smaller solvent molecule than cyclohexane.

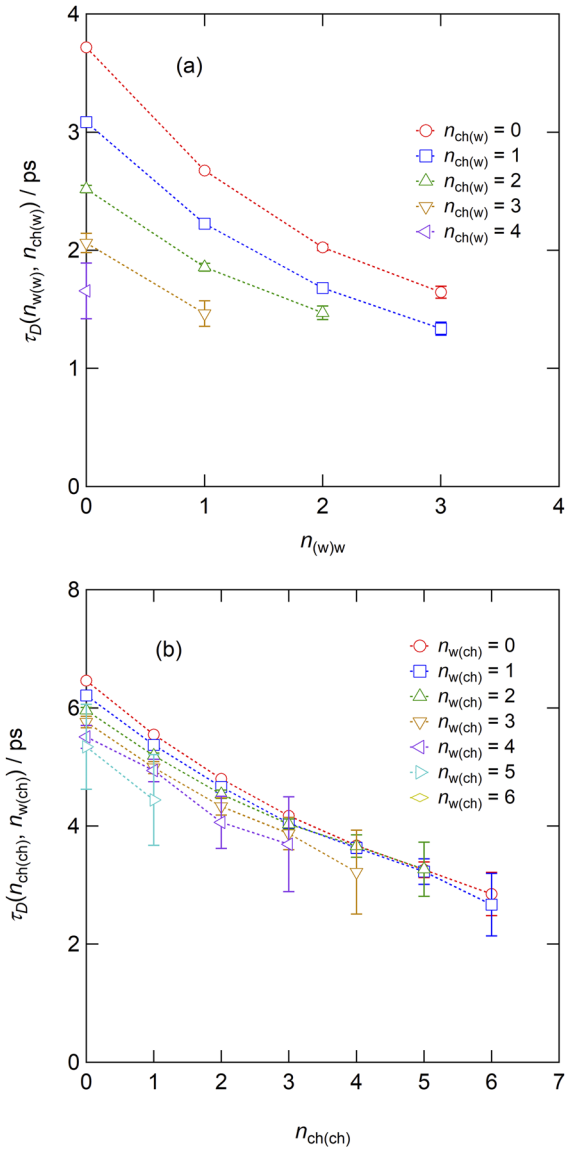

FIG. 3. (a) Velocity relaxation time $\tau_D(n_{w(w)}, n_{ch(w)})$ for water as a function of the number $n_{w(w)}$ of solvating water molecules. (b) The velocity relaxation time $\tau_D(n_{ch(ch)}, n_{w(ch)})$ for cyclohexane as a function of the number $n_{ch(ch)}$ of solvating cyclohexane molecules. The thermodynamic state is at 1.0 M, 400 °C, and x_w = 0.5.

The conditioned velocity relaxation time for cyclohexane $\tau_D(n_{ch(ch)}, n_{w(ch)})$ is shown in Fig. 3(b). The τ_D values for cyclohexane also decrease as either $n_{ch(ch)}$ or $n_{w(ch)}$ increases, and the effect of $n_{ch(ch)}$ is much stronger on the τ_D of cyclohexane. The reductions in τ_D for unit increases of $n_{ch(ch)}$ and $n_{w(ch)}$ are 10%–15% and 3%–4%, respectively. This trend agrees with the simple kinetic theory of gases, indicating that collisions with species of larger mass and larger cross sections lead to greater reductions in the self-diffusion coefficients. It is noted that the impact of solvating cyclohexane molecules on cyclohexane diffusion is smaller than the impact of solvating water molecules on water diffusion. This highlights the significant dynamic effects of interactions between attracting pairs of water molecules on water self-diffusion.

The results at a higher density of 4.0 M are shown in Fig. 4 with the temperature and water content fixed at θ = 400 °C and x_w = 0.5, respectively. The trends observed at 4.0 M are similar to those seen at 1.0 M. At higher density, the conditioned velocity autocorrelation can be sampled over a wider range of solvation structures, including a more crowded solvation shell comprising a larger number of solvating molecules. Thus, we can examine the dependency of the velocity relaxation time for different combinations of the solute and solvent. Figures 4(a) and 4(b) plot the τ_D values for water and cyclohexane, respectively, against the self-solvation number. The plots in (a) at fixed $n_{ch(w)}$ exhibit a downward convex curve against $n_{w(w)}$, while the plots in (b) at fixed $n_{w(ch)}$ are nearly linear against $n_{ch(ch)}$. This suggests that the impact of an addition of a water solvent molecule to the solvation shell becomes smaller when there are more water molecules that already exist in a neighbor. In contrast, for cyclohexane, the impact of one cyclohexane solvent molecule in a crowded shell is similar to that in a shell containing fewer

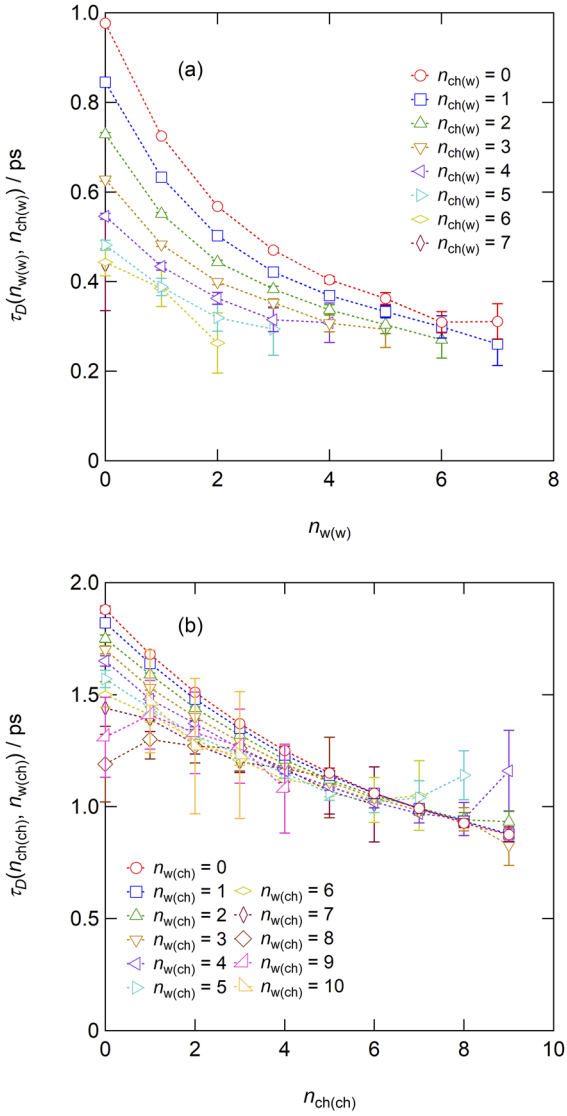

FIG. 4. (a) Velocity relaxation time $\tau_D(n_{w(w)}, n_{ch(w)})$ for water as a function of the number $n_{w(w)}$ of solvating water molecules. (b) The velocity relaxation time $\tau_D(n_{ch(ch)}, n_{w(ch)})$ for cyclohexane as a function of the number $n_{ch(ch)}$ of solvating cyclohexane molecules. The thermodynamic state is at 4.0 M, 400 °C, and x_w = 0.5.

cyclohexane solvent molecules. This difference between water and cyclohexane suggests that the interactions between solute and solvent water are more correlated when a larger number of water molecules are present in the solvation shell. In contrast, the solute–solvent binary interactions between cyclohexane molecules are more uncorrelated and isolated from each other.

The interactions between a pair of water molecules are attractive and persistent over a finite period. Therefore, the additional interactions with the incoming partner solvent may compete with the preexisting interactions, especially when the diffusing solute is subject to attractive forces and torques from multiple orientations. The attraction between a neighboring pair of solvating molecules within the solvation shell may also weaken the influence of each solvent molecule in the solvation shell at larger solvation numbers. This is because the presence of neighboring candidates as H-bonding partners for a particular solvent molecule other than what the diffusing solute can serve as a distraction and disturbance for H-bonding between a solute–solvent pair. The H-bonding between a specific pair of water molecules is more effective when the water pair is more isolated.[13,14,17] On the other hand, the linearity of τ_D against $n_{ch(ch)}$ for cyclohexane suggests that interactions between cyclohexane molecules are short-lived collision-like encounters that are uncorrelated with successive interactions. As a result, the effects of an increased frequency of interactions can be additive up to a fairly large $n_{ch(ch)}$ value. The dependency of τ_D on the cross-solvation numbers for water and cyclohexane ($n_{ch(w)}$ and $n_{w(ch)}$, respectively) more closely resembles that between cyclohexane around cyclohexane rather than that between water and water. This can be expected from the weaker interactions between contact pairs of water and cyclohexane than H-bonding. The τ_D values are plotted against the cross-solvation numbers $n_{ch(w)}$ and $n_{w(ch)}$ in Fig. S6; the plots are nearly linear and do not exhibit much of a downward convex curve.

We now discuss the relationship between the translational relaxation time τ_D and the relaxation time of the solvation shell τ_S with the goal of understanding the extent to which the translational diffusion is confined within the solvation shell and the extent to which the memory of the translational velocity extends beyond the lifetime of the solvation shell. Figure 5 shows a contour plot of the ratio $\tau_D(m,n)/\tau_S(m,n)$ as a function of the self- and cross-solvation numbers for θ = 400 °C, ρ = 4.0 M, and x_w = 0.5. Here, the ratio τ_D/τ_S measures the extent of velocity relaxation within the solvation shell. Smaller and larger values of τ_D/τ_S, respectively, indicate in-shell and mobile-shell types of self-diffusion, as described in Sec. II B. For both water in (a) and cyclohexane in (b), there is a region of states for the solvation shell that is represented by self- and cross-solvation numbers where the ratio $\tau_D(m,n)/\tau_S(m,n)$ is significantly larger than unity. This region roughly corresponds to where probabilities of occurrence of solvation states are relatively large. The contour plot of the probability of occurrence at the same thermodynamic state is shown in Figs. S3(e) and S3(f). In the outer periphery of this region, where the probability of occurrence declines toward zero as either the self- or cross-solvation number increases, the ratio $\tau_D(m,n)/\tau_S(m,n)$ sharply decreases toward zero. The decrease in $\tau_D(m,n)/\tau_S(m,n)$ is primarily due to the increase in $\tau_S(m,n)$ in conditions where rare dense clustering in the thermodynamic state occurs, as examined in Sec. III A. The decrease in $\tau_D(m,n)$ is also due to the smaller $\tau_D(m,n)$ resulting from the crowded solvation shell, as discussed above. The ratio $\tau_D(m,n)/\tau_S(m,n)$ for cyclohexane is much larger than that for water because the self-diffusion of cyclohexane that is surrounded by more water molecules tends to be more mobile-shell type, as discussed below.

To examine how the ratio τ_D/τ_S depends on the thermodynamic variables x_w, ρ, and T, we obtain the bulk value of τ_D/τ_S at each specific thermodynamic state. Here, τ_D and τ_S are weighted sums of the conditioned relaxation time [Eq. (8)]. The obtained τ_D/τ_S values are plotted against x_w in Fig. 6. The τ_D/τ_S for cyclohexane largely increases with x_w. Thus, cyclohexane is of the least mobile-shell type in pure cyclohexane and becomes more of the

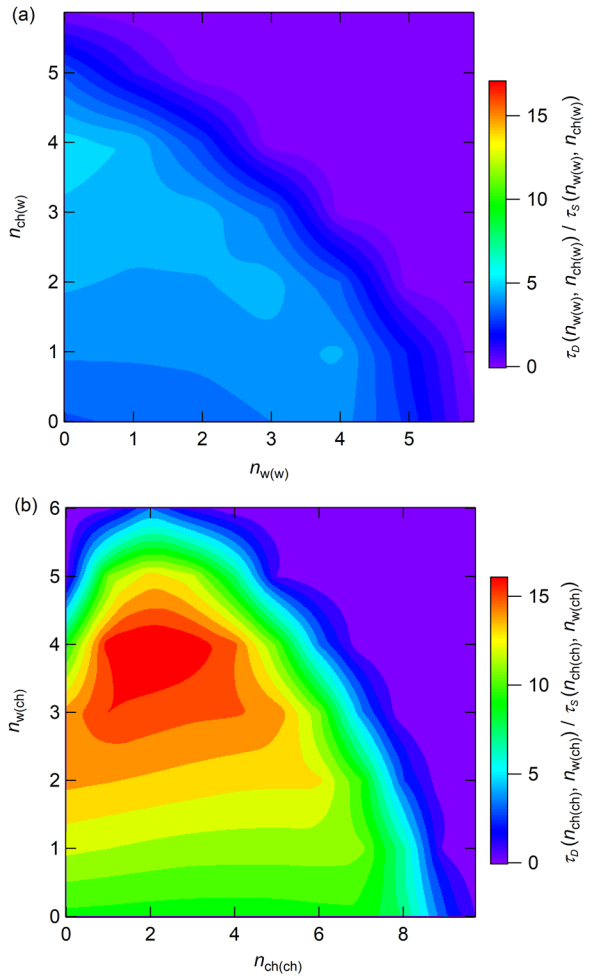

FIG. 5. (a) Contour plot of the ratio $\tau_D(n_{w(w)}, n_{ch(w)})/\tau_S(n_{w(w)}, n_{ch(w)})$ for water as a function of the self- and cross-solvation numbers $n_{w(w)}$ and $n_{ch(w)}$. (b) The contour plot of the ratio $\tau_D(n_{ch(ch)}, n_{w(ch)})/\tau_S(n_{ch(ch)}, n_{w(ch)})$ for cyclohexane as a function of the self- and cross-solvation numbers $n_{ch(ch)}$ and $n_{w(ch)}$. The thermodynamic state is at 4.0 M, 400 °C, and x_w = 0.5. In the region corresponding to large solvation numbers where the probability of occurrence is too small to evaluate the conditioned τ_D/τ_S values, the contour plot is filled with the value of zero.

mobile-shell type as the water content increases. When a cyclohexane molecule is surrounded by water in a binary mixture, the solvation state of the diffusing cyclohexane molecule tends to vary due to the weak interactions between water and cyclohexane and the fast motion of water molecules. Thus, the diffusing cyclohexane molecules cannot be kept inside the solvation shell, and this mobility is enhanced as the water content increases. This results in the local separation of water and cyclohexane in binary mixtures, which is microscopically inhomogeneous although macroscopically homogeneous.[13] Compared to cyclohexane, the τ_D/τ_S value of water is much less dependent on x_w and only slightly increases with x_w. The contribution of the surrounding water molecules to their solvation states is controlled primarily by H-bonding interactions, which are

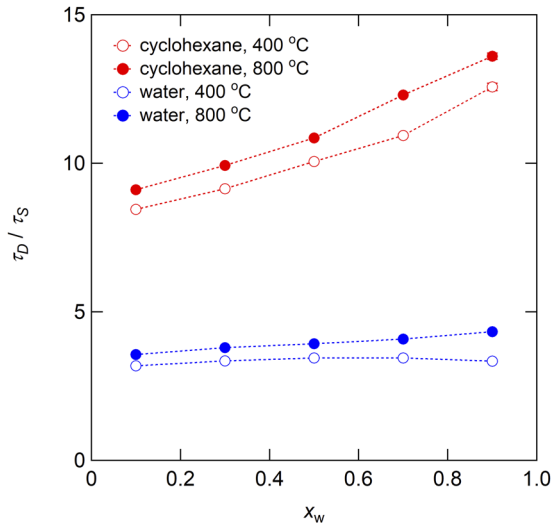

FIG. 6. Ratios τ_D/τ_S for water and cyclohexane at ρ = 1.0 M as plotted as functions of x_w.

effective at both high and low water contents. Although cyclohexane molecules as a solvent around water are only weakly attracted to the solute water, the residence time is comparable to that of water molecules that are H-bonded to the solute due to the slower motion of cyclohexane. Increasing the temperature causes the self-diffusion to become more mobile-shell type for both water and cyclohexane, as seen in Fig. 6.

C. Rotational dynamics

To further investigate the dynamic interactions in supercritical mixtures of water and cyclohexane, we turn our focus to rotational dynamics. As the rotational dynamics are short-ranged and sensitive to the orientational preferences of the intermolecular interactions,[10,14] it is valuable to explore the differences in rotational dynamics between polar water and nonpolar cyclohexane. Here, we examine the rotational dynamics based on the second-order reorientational relaxation time τ_{2R} of the O–H axis of water and the C–H axis of cyclohexane. The solvation-number-conditioned reorientational relaxation time is shown in Fig. 7 at 400 °C, 1.0 M, and x_w = 0.5. The results for water are shown in Fig. 7(a), and the τ_{2R} values at each $n_{ch(w)}$ are plotted against $n_{w(w)}$. Notably, in contrast to the conditioned τ_D in the same thermodynamic state (Fig. 3), the τ_{2R} value for water depends only on $n_{w(w)}$ and is nearly independent of $n_{ch(w)}$. The τ_{2R} value for water increases with $n_{w(w)}$ starting at $n_{w(w)}$ = 1 because the orientation of the solute water molecule is maintained when it forms more H-bonds with the surrounding water molecules. The τ_{2R} value at $n_{w(w)}$ = 0 is exceptionally large due to the effects of free rotation. These trends in τ_{2R} with respect to $n_{w(w)}$ are common to supercritical water as a one-component system.[10,14] Thus, the rotation of water is nearly independent of the presence of neighboring cyclohexane molecules in the solvation shell. The rotational motion proceeds more locally in space than the translational diffusion, which extends to a wider space beyond the solvation shell. Thus, the exclusive volume due to cyclohexane has a limited ability to hinder water rotation. The τ_{2R} values for water have little

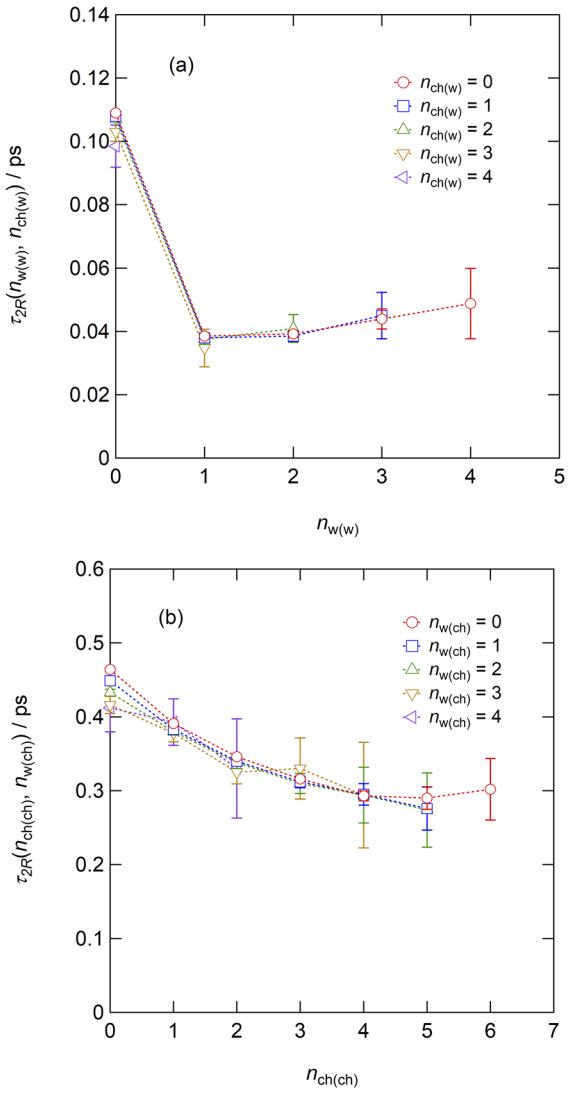

FIG. 7. (a) Reorientational correlation time $\tau_{2R}\left(n_{w(w)}, n_{ch(w)}\right)$ for water as a function of the number $n_{w(w)}$ of solvating water molecules. (b) The velocity relaxation time $\tau_{2R}\left(n_{ch(ch)}, n_{w(ch)}\right)$ for cyclohexane as a function of the number $n_{ch(ch)}$ of solvating cyclohexane molecules. The thermodynamic state is at 1.0 M, 400 °C, and x_w = 0.5.

dependence on $n_{ch(w)}$ at a higher density of 4.0 M (Fig. S7), where interactions between water and cyclohexane are much more frequent. This means that the collisional interactions between solute water molecules and solvating cyclohexane molecules have a limited ability in altering the orientation of the solute water molecules because of the weak electrostatic interactions between water and cyclohexane.

The τ_{2R} values for cyclohexane are plotted in Fig. 7(b) at 400 °C, 1.0 M, and x_w = 0.5. As in the case of water, the reorientational motion of cyclohexane is controlled primarily by other cyclohexane molecules, while it is nearly unaffected by water molecules. However, in contrast to the results shown for water in Fig. 7(a), τ_{2R} decreases with increasing $n_{ch(ch)}$ for cyclohexane [Fig. 7(b)]. This means that cyclohexane molecules in the solvation shell randomize the orientation of the solute cyclohexane molecule, in contrast to water, where the solvent water molecules attract the solute water molecule via H-bonding to maintain its orientation. The interactions between cyclohexane molecules are uncorrelated collisions with respect to translational diffusion but can flip the neighboring solute cyclohexane molecules, altering their orientations. While the interactions between cyclohexane and water are also collisional, the effects of water on cyclohexane reorientation are small due to the smaller mass and size of water; thus, these effects are not distinguishable in the resultant correlation time.

The ratio $\tau_{2R}(m,n)/\tau_S(m,n)$ for the conditional correlation times is shown in the contour plot in Fig. S8. As is the case for the self-diffusion, the $\tau_{2R}(m,n)/\tau_S(m,n)$ values are significantly greater than zero in the region of the solvation states with relatively high probabilities of occurrence. The $\tau_{2R}(m,n)/\tau_S(m,n)$ values decrease as the self- and cross-solvation numbers increase due to the increased lifetime of the solvation shell in the more crowded shells. The $\tau_{2R}(m,n)/\tau_S(m,n)$ values are smaller than the $\tau_D(m,n)/\tau_S(m,n)$ values due to the short-ranged and short-lived in-shell characteristics of the rotational dynamics. It should be noted that the color scale in Fig. S8 for $\tau_{2R}(m,n)/\tau_S(m,n)$ is expanded compared to that in Fig. 5 for $\tau_D(m,n)/\tau_S(m,n)$. The ratio τ_{2R}/τ_S of the bulk correlation times is plotted against x_w in Fig. S9, while the values of τ_{2R} and τ_S are shown in Figs. S10(a) and S10(b), respectively. The bulk τ_{2R}/τ_S values for water and cyclohexane are both less than unity, indicating in-shell-type dynamics due to the fast rotation at such high temperatures. The τ_{2R}/τ_S values of water are small at large x_w because the less-packed conditions lead to a relatively small τ_{2R} value and a relatively large τ_S value. At a fixed ρ value, the space becomes less packed with increasing x_w due to the smaller molecular size of water compared to cyclohexane. The rotation of cyclohexane is less of the in-shell type compared to water because of the larger moment of inertia and more changeable structure of the solvation shell for cyclohexane.

D. Activation energy for self-diffusion

In a previous study,[13] we determined the activation energies E_a for the self-diffusion of water and cyclohexane using high-temperature NMR experiments. The dependence of E_a on the thermodynamic state has been examined based on the formulation of D as a function of T, ρ, and x_w developed along with systematic MD simulations over a wide range of thermodynamic states. The most remarkable difference in E_a between water and cyclohexane lies in its dependence on x_w. The E_a for water ($E_{a,w}$) largely increases with x_w, while the E_a for cyclohexane ($E_{a,ch}$) is nearly independent of x_w. The increase in $E_{a,w}$ with x_w implies that at high water contents, the H-bonds with neighboring water molecules create a barrier to the self-diffusion of water. Nevertheless, a direct examination of the dependence of E_a on the state of the solvation shell is needed. To go beyond examinations as a function of the bulk parameters (e.g., T, ρ, and x_w), we scrutinize the dependence of $E_{a,w}$ and $E_{a,ch}$ on the local solvation states, as represented by the self- and cross-solvation numbers. The solvation-number-conditioned self-diffusion coefficient $D_{m,n}$ can be obtained from $\tau_D(m,n)$ through the relationship

$D_{m,n} = RT\tau_D(m,n)/M$, where R is the gas constant and M is the molar mass of the diffusing solute molecule. This is equivalent to obtaining $D_{m,n}$ using the Green–Kubo relation for the conditioned velocity autocorrelation function. The conditioned activation energy $E_a(m,n)$ is given by

$$E_a(m,n) = -R\frac{\partial \ln D_{m,n}}{\partial\left(\frac{1}{T}\right)}. \quad (9)$$

The sum rule for the decomposed properties [cf. Eq. (8)] can be expressed in the case of $E_a(m,n)$ as

$$E_a = \sum_m \sum_n P_{m,n} E_a(m,n). \quad (10)$$

As E_a is a derivative property and has a large uncertainty, we first verify the validity of the sum rule in Eq. (10) for the present discussion, as shown in Fig. S11.

The $E_{a,w}$ values plotted in Fig. 8(a) show that $E_{a,w}$ markedly increases with increasing $n_{w(w)}$, as expected from the large values of the unconditioned bulk $E_{a,w}$ for large x_w. The $E_{a,w}$ value increases with $n_{ch(w)}$ in addition to $n_{w(w)}$, although the effect of $n_{ch(w)}$ is much weaker. The increases in $E_{a,w}$ per unit increase in $n_{w(w)}$ and $n_{ch(w)}$ are 2 and 0.4 kJ mol^{-1}, respectively. The effect of $n_{ch(w)}$ is attributed to the van der Waals interaction between water and cyclohexane, which is modeled by the Lennard-Jones potential in the current classical MD simulations. An increase in $n_{ch(w)}$ contributes to the reduction in $E_{a,w}$ with x_w due to the reduction in the number of neighboring cyclohexane molecules around the water molecule. However, the impact of $n_{w(w)}$ is overwhelming, and the bulk $E_{a,w}$ value increases with increasing x_w overall. There are a few exceptional conditions: a slight decrease in $E_{a,w}$ is observed for $(n_{w(w)}, n_{ch(w)}) = (2, 3)$, and the rate of increase in x_w declines at $(n_{w(w)}, n_{ch(w)}) = (3, 1)$. Similar trends are observed at a higher water content [$x_w = 0.9$ and $n_{w(w)} = 3$ and 4; Fig. S12 (c)]. These conditions correspond to solvation states with relatively large $n_{w(w)}$ for each thermodynamic state. The observed decrease in $E_{a,w}$ suggests that when a diffusing water molecule gathers extra water molecules around it, the interactions between the solute and solvent water molecules are weakened. This is likely because the extra water molecules enable the solute and the solvent water molecules to more easily exchange with each other and reorganize the H-bonding. This agrees with the previous observation that the H-bonding is strengthened when a pair of water molecules is isolated by either coexisting hydrophobic cyclohexane or a void at low density.[13] At large $n_{ch(w)}$, the decrease in $E_{a,w}$ occurs at smaller $n_{w(w)}$, indicating that the space available for solvent water molecules in the solvation shell is more restricted when the solvation shell contains more cyclohexane molecules. This results in the "saturation" of solvent water molecules at low water contents.

The $E_{a,ch}$ values plotted in Fig. 8(b) show that $E_{a,ch}$ increases with increasing $n_{ch(ch)}$; however, the increase in $E_{a,ch}$ per unit $n_{ch(ch)}$ is only 0.5 kJ mol^{-1}, much smaller than that for $E_{a,w}$. This highlights the extraordinarily large influence of water–water attractive interactions on self-diffusion. Thus, the effects of surrounding cyclohexane molecules on E_a as a solvent in the solvation shell of a diffusing cyclohexane molecule are similar to the effects of a solvation shell of diffusing water molecules. The increase in $E_{a,ch}$ per unit $n_{w(ch)}$ is only 0.2 kJ mol^{-1}, with the exceptions of larger $n_{ch(ch)}$ and $n_{w(ch)}$ conditions such as $(n_{ch(ch)}, n_{w(ch)}) = (6, 0)$, (4, 3), (2, 4), and (1, 5), for which the $E_{a,ch}$ values are noticeably larger than those in other conditions; even though the error bars are large in these conditions because of the small probabilities of occurrence, the trend pointed out here is probable because the increase in $E_{a,ch}$ is observed in multiple conditions. The impact of encountering surrounding water molecules is typically small as long as the interactions between the solute cyclohexane and solvent water molecules are uncorrelated collisions. Only on rare occasions (when the water and cyclohexane molecules are highly crowded, strengthening the H-bonding interactions between the water molecules) does the

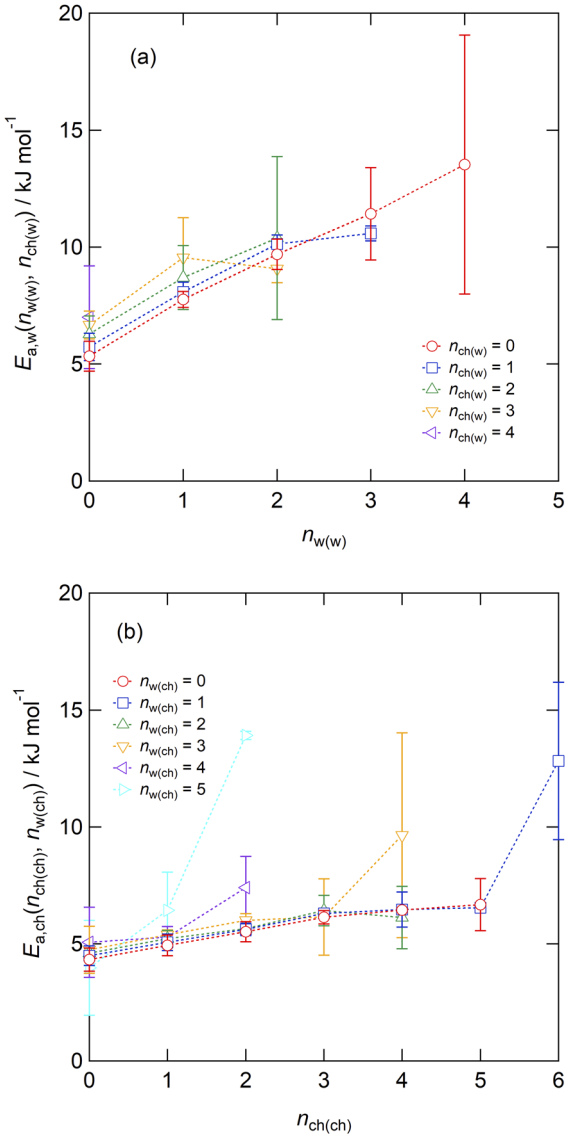

FIG. 8. (a) Solvation-number-conditioned activation energy $E_{a,w}(n_{w(w)}, n_{ch(w)})$ for water as a function of the number $n_{w(w)}$ of solvating water molecules at 1.0 M and $x_w = 0.5$. (b) The solvation-number-conditioned activation energy $E_{a,ch}(n_{ch(ch)}, n_{w(ch)})$ for cyclohexane as a function of the number $n_{ch(ch)}$ of solvating cyclohexane molecules at 1.0 M and $x_w = 0.5$.

formation of such microscopic environments create a high barrier for cyclohexane diffusion. The conditions where such enhancements in E_a are observed correspond to the case where the solvation shell is formed by highly clustered solvents, resulting in a long lifetime τ_S. The probabilities of occurrence for such clusters are so low that this scenario does not affect the overall bulk $E_{a,ch}$ value. Nevertheless, the occurrence of such clusters may be responsible for rare barrier-crossing events such as chemical reactions of hydrophobic species and supercritical water reactions, which should be further investigated.

IV. CONCLUSIONS

The microscopic molecular dynamics of the self-diffusion of water and cyclohexane in their binary mixtures were studied by examining how the structure and lifetime of the solvation shell control the relaxation time of the translational velocity τ_D. The decomposition scheme for bulk τ_D based on the self- and cross-solvation numbers showed that the factor with the strongest effect on the self-diffusion of water is H-bonding between water molecules; solvent cyclohexane molecules exhibit a moderate effect on both solute water and solute cyclohexane molecules, while the weakest effect was observed for solvent water molecules on the self-diffusion of solute cyclohexane molecules. The impact of solvent water molecules on solute water molecules is larger when there are fewer water molecules in the solvation shell and weakens as the number of water molecules in the shell increases. This suggests the existence of strong H-bonding between isolated pairs of water molecules and more frequent reorganization of H-bonds in shells filled with more water molecules. The effects of cyclohexane as a solvent on both water and cyclohexane solute molecules are nearly independent of the number of cyclohexane molecules in the solvation shell. This reflects the characteristics of the interactions of cyclohexane molecules with either cyclohexane or water molecules in contact as the interactions between different contact pairs are more collisional and uncorrelated than the interactions between pairs of the same species. This reflects that the interactions of cyclohexane molecules with either cyclohexane or water molecules are more collisional and uncorrelated than the interactions between a pair of water molecules. These dynamics of cyclohexane are further corroborated by examining the rotational dynamics, revealing that the free rotation of cyclohexane molecules is independent of the solvation shell. Such isolation of the interactions of cyclohexane is in sharp contrast to the interactions of water, which are more collective and extend for a finite time due to attractive interactions between water molecules. The self-diffusion of both water and cyclohexane is of the mobile-shell type, which means that the structure of the solvation shell decays faster than the memory of the translational velocity; thus, the self-diffusing molecules migrate across the solvation shell. We found that cyclohexane molecules in water show much more significant mobile-shell-type behaviors than water molecules, and these behaviors are enhanced at high water contents. This means that the hydration structures around cyclohexane are less stable than those around water, and solute cyclohexane molecules tend to diffuse out of the surrounding water molecules. This diffusion is aided by the congregation of water molecules with each other and results in the transient preferential association between molecules of the same species, which causes microscopic inhomogeneity. In the solvation states where the shell is the most crowded for a given thermodynamic state, the lifetime of the solvation shell becomes remarkably long, and the self-diffusion is more confined. The activation energy of self-diffusion in such a crowded shell is larger than that in the average shell. When considering the self-diffusion coefficients, the contributions of these rare crowded shells have little effect on the average weighted sum of the self-diffusion coefficient that corresponds to the experimental observable. Nevertheless, the molecular mechanism of such long-lived confinement for a solute in a solvation shell could be related to rare events such as chemical reactions, which are often of great importance from the perspectives of both fundamental science and practical applications.

SUPPLEMENTARY MATERIAL

See the supplementary material for the data values and plots that are not included in this paper.

ACKNOWLEDGMENTS

This study was supported by Grants-in-Aid for Scientific Research (Grant Nos. 17K05754 and 20K05433) from the Japan Society for the Promotion of Science (JSPS). Numerical calculations were performed using the Research Center for Computational Science, Okazaki, Japan.

DATA AVAILABILITY

The data that support the findings of this study are available within this article and from the corresponding author upon reasonable request.

REFERENCES

[1] N. Akiya and P. E. Savage, Chem. Rev. **102**, 2725 (2002).
[2] H. Weingärtner and E. U. Franck, Angew. Chem., Int. Ed. **44**, 2672 (2005).
[3] C. Rodriguez Correa and A. Kruse, J. Supercrit. Fluids **133**, 573 (2018).
[4] M. Kubo, T. Takizawa, C. Wakai, N. Matubayasi, and M. Nakahara, J. Chem. Phys. **121**, 960 (2004).
[5] K. Yoshida, C. Wakai, N. Matubayasi, and M. Nakahara, J. Phys. Chem. A **108**, 7479 (2004).
[6] H. Kimura, M. Hirayama, K. Yoshida, Y. Uosaki, and M. Nakahara, J. Phys. Chem. A **118**, 1309 (2014).
[7] P. R. Alburquerque, B. R. Ramachandran, T. Junk, and T. N. V. Karsili, J. Phys. Chem. A **124**, 2530 (2020).
[8] K. Yoshida, H. Yoshioka, N. Ushigusa, and M. Nakahara, Chem. Lett. **50**, 316 (2021).
[9] N. Matubayasi, C. Wakai, and M. Nakahara, J. Chem. Phys. **107**, 9133 (1997).
[10] N. Matubayasi, N. Nakao, and M. Nakahara, J. Chem. Phys. **114**, 4107 (2001).
[11] K. Yoshida, C. Wakai, N. Matubayasi, and M. Nakahara, J. Chem. Phys. **123**, 164506 (2005).
[12] K. Yoshida, N. Matubayasi, and M. Nakahara, J. Chem. Phys. **129**, 214501 (2008).
[13] K. Yoshida and M. Nakahara, J. Chem. Phys. **150**, 174505 (2019).
[14] K. Yoshida, N. Matubayasi, and M. Nakahara, J. Chem. Phys. **127**, 174509 (2007).
[15] K. Yoshida, N. Matubayasi, and M. Nakahara, J. Chem. Phys. **125**, 074307 (2006).
[16] K. Yoshida, N. Matubayasi, and M. Nakahara, J. Mol. Liq. **147**, 96 (2009).
[17] N. Matubayasi, C. Wakai, and M. Nakahara, J. Chem. Phys. **110**, 8000 (1999).

[18]K. Yoshida, N. Matubayasi, Y. Uosaki, and M. Nakahara, J. Chem. Phys. **137**, 194506 (2012).
[19]K. Yoshida, N. Matubayasi, Y. Uosaki, and M. Nakahara, J. Chem. Phys. **138**, 134508 (2013).
[20]I. Skarmoutsos and E. Guardia, J. Chem. Phys. **132**, 074502 (2010).
[21]H. Ma, J. Chem. Phys. **136**, 214501 (2012).
[22]G. Raabe and R. J. Sadus, J. Chem. Phys. **137**, 104512 (2012).
[23]G. Galli and D. Pan, Proc. Natl. Acad. Sci. U. S. A. **110**, 6250 (2013).
[24]C. J. Sahle, C. Sternemann, C. Schmidt, S. Lehtola, S. Jahn, L. Simonelli, S. Huotari, M. Hakala, T. Pylkkänen, A. Nyrow, K. Mende, M. Tolan, K. Hämäläinen, and M. Wilke, Proc. Natl. Acad. Sci. U. S. A. **110**, 6301 (2013).
[25]I. Skarmoutsos, E. Guardia, and J. Samios, J. Supercrit. Fluids **130**, 156 (2017).
[26]A. Choudhary and A. Chandra, J. Chem. Phys. **151**, 044508 (2019).
[27]G. Ng Pack, M. C. Rotondaro, P. P. Shah, A. Mandal, S. Erramilli, and L. D. Ziegler, Phys. Chem. Chem. Phys. **21**, 21249 (2019).
[28]N. Dasgupta, Y. K. Shin, M. V. Fedkin, and A. van Duin, J. Chem. Phys. **152**, 204502 (2020).
[29]R. Hou, Y. Quan, and D. Pan, J. Chem. Phys. **153**, 101103 (2020).
[30]P. Sun, J. B. Hastings, D. Ishikawa, A. Q. R. Baron, and G. Monaco, Phys. Rev. Lett. **125**, 256001 (2020).
[31]C. Andreani, G. Romanelli, A. Parmentier, R. Senesi, A. I. Kolesnikov, H.-Y. Ko, M. F. Calegari Andrade, and R. Car, J. Phys. Chem. Lett. **11**, 9461 (2020).
[32]H. J. C. Berendsen, J. R. Grigera, and T. P. Straatsma, J. Phys. Chem. **91**, 6269 (1987).
[33]W. L. Jorgensen and D. L. Severance, J. Am. Chem. Soc. **112**, 4768 (1990).
[34]P. B. Balbuena, K. P. Johnston, P. J. Rossky, and J.-K. Hyun, J. Phys. Chem. B **102**, 3806 (1998).
[35]M. S. Skaf and D. Laria, J. Chem. Phys. **113**, 3499 (2000).
[36]T. Ohmori and Y. Kimura, J. Chem. Phys. **119**, 7328 (2003).
[37]N. Matubayasi and M. Nakahara, J. Chem. Phys. **122**, 074509 (2005).
[38]D. T. Kallikragas, A. Y. Plugatyr, and I. M. Svishchev, J. Chem. Eng. Data **59**, 1964 (2014).
[39]A. Choudhary and A. Chandra, J. Phys. Chem. B **119**, 8600 (2015).
[40]Y. Guissani and B. Guillot, J. Chem. Phys. **98**, 8221 (1993).
[41]W. Wagner and A. Pruß, J. Phys. Chem. Ref. Data **31**, 387 (2002).
[42]Revised Release on the IAPWS Formulation 1995 for the Thermodynamic Properties of Ordinary Water Substance for General and Scientific Use, URL: http://www.iapws.org, 2016.
[43]B. Hess, C. Kutzner, D. van der Spoel, and E. Lindahl, J. Chem. Theory Comput. **4**, 435 (2008).